

# A Novel Computational Imaging Method Using Reconfigurable Intelligent Surfaces

Kavian Zirak<sup>(1)</sup> and Mohammadreza F. Imani<sup>(1)</sup>

(1) Arizona State University, Tempe, AZ 85287, USA ([kzirak@asu.edu](mailto:kzirak@asu.edu), [Mohammadreza.Imani@asu.edu](mailto:Mohammadreza.Imani@asu.edu))

**Abstract**—This paper proposes and numerically demonstrates a novel method for computational imaging using reconfigurable intelligent surfaces (RISs) that combines the benefits of compressive imaging using random patterns with spotlight imaging. In our approach, RISs are programmed to direct their beams toward a region of interest (ROI) where they interfere with each other, resulting in spatially diverse patterns that can multiplex the information within the ROI into a few measurements. Since each RIS produces a directive beam, the resulting speckle pattern is only confined to near the ROI, helping to reduce clutter, a typical issue with using random patterns. Furthermore, our method requires fewer measurements than raster scanning and can work even when RISs are separated, which is useful in practical implementation. The proposed RIS-enabled imaging system can find applications in security screening, user tracking, and activity recognition.

**Keywords**—Metasurfaces; Microwave Imaging.

## I. INTRODUCTION

Reconfigurable intelligent surfaces (RISs) have gained traction due to their ability to sculpt desired wireless communication systems [1]. RISs are electrically large surfaces with many resonant reflectors that can redirect signals in arbitrary directions, avoiding signal blockage, mitigating interference, or avoiding jammers. These electrically large apertures and their ability to form prescribed reflection patterns can also be advantageous for imaging and sensing. They can realize the desired spatial resolution while mitigating the need for moving antennas or complex switch arrays. Further, the transmitter and receiver of an RIS-enabled imaging system can be placed close together, making temporal and phase synchronization easier.

Most previous works on RIS-enabled imaging primarily utilized RIS to generate random patterns combined with computational imaging techniques. For example, random patterns have been applied with artificial neural networks to perform human imaging and vital sign recognition [2]. However, random patterns result in signals transmitted in all directions, increasing clutter in imaging and causing interference for other devices. Other works have used RISs to generate raster-scanned directive beams for imaging [3], eliminating clutter and interference concerns. This method is also constrained since it requires many measurements with precise beamforming.

This paper introduces a new approach to RIS-enabled computational imaging that combines the benefits of random patterns with spotlight imaging. Inspired by radar coincident imaging [4], we direct signals from various RISs toward an ROI, where the interference of these beams creates a speckle

pattern that allows for multiplexing information across the ROI. By adjusting the beams' characteristics, different speckle patterns can be generated. We can then reconstruct reflectivity maps through computational processing of the collected return signals. In this paper, we use numerical models in MATLAB to demonstrate this method's superior performance compared to random patterns or raster scanning.

## II. RESULTS

The overall configuration of the imaging problem considered here is shown in Fig. 1. Here, we assume one transmitter that illuminates 6 RISs that redirect their signals toward an ROI. The receiver, co-located with the transmitter, utilizes another 6 RISs to collect the signal scattered by the objects in the ROI. We have developed a numerical code to analyze various imaging methods possible in this geometry. For demonstration purposes, each RIS is assumed to consist of  $20 \times 20$  elements with a resonance frequency of 6 GHz and a spacing of 2 cm ( $L_x = L_y = 40\text{cm}$ ). We assume each element is loaded by a varactor diode, which allows the reflected phase to be continuously tuned. The element-element coupling and losses are ignored for simplicity. The transmitter and receiver are positioned at ( $x = 0, y = -3\text{ m}, z = 3\text{ m}$ ), emitting a spherical wave towards a  $2 \times 3$  array of RISs contained within an area of ( $0 < x < 80\text{cm}, 30\text{cm} < y < 150\text{cm}, z = 0$ ). The receiver RISs follow the same configuration but are mirrored with respect to the zy-plane, as shown in Fig. 1.

In our proposed method, each RIS is designed to direct the beam within the ROI, allowing the beams from different RISs to interfere constructively or destructively. However, the exact redirection angles are not fixed; they can vary slightly while remaining within the ROI. The elements of each RIS can also reflect the beam with different phases from other RISs. This variation in the beam direction, its phase, and frequency can change the speckle patterns formed at the ROI. Each specific arrangement of redirection angles and phase offset for the 6 RISs will be referred to as a *mask* for brevity. The masks used for transmitting and receiving RISs will also be different. Fig. 2 shows the speckle pattern for different masks and frequencies. The spatial distribution of the patterns interrogating the ROI changes as the mask or frequency is altered, allowing for multiplexing the spatial information into a few measurements indexed by frequency and/or masks.

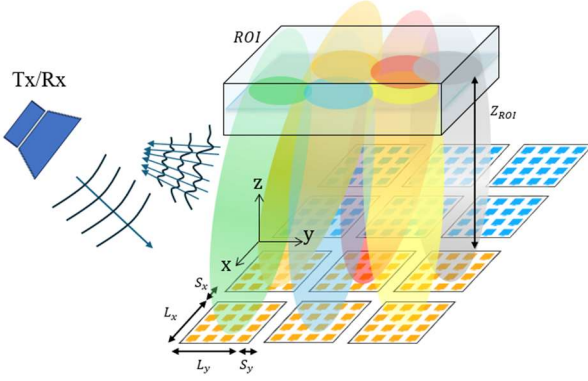


Figure 1: The configuration of the imaging problem considered in this paper.

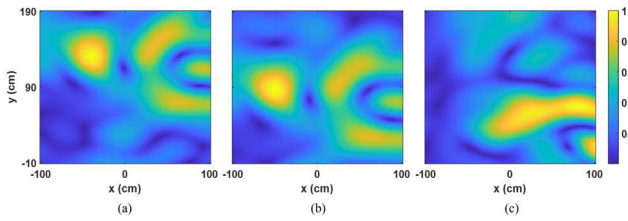


Figure 2: The speckle pattern at  $z=8m$  for different masks and frequencies. (a) mask 1 at 6 GHz, (b) mask 1 at 5.6 GHz, and (c) mask 2 at 6 GHz

The numerical model divides the imaging problem into forward and inverse problems [5]. In the forward problem, using the First-Born approximation for the objects, we compute the return signal collected by the receiver, denoted as  $\mathbf{g}_{M \times 1}$ , in which  $M$  is the number of measurements equal to the product of the number of frequency points and the number of masks. In the inverse problem, we use  $\mathbf{g}$  to estimate the target's reflectivity maps. To do that, we define an ROI around the object that is discretized into  $N$  voxels. We can then compute a sensing matrix,  $\mathbf{H}$ , that relates the reflectivity map of those voxels to the return signal in the following manner:

$$\mathbf{g}_{M \times 1} = \mathbf{H}_{M \times N} \boldsymbol{\sigma}_{N \times 1}, \quad (1)$$

where  $\boldsymbol{\sigma}_{N \times 1}$  is the reflectivity map for the  $N$  voxels of the ROI. The sensing matrix element  $h(i, j)$  is computed as  $h(i, j) = \bar{E}_{Tx}^i(\vec{r}_j) \cdot \bar{E}_{Rx}^i(\vec{r}_j)$ , where  $i$  refers to the  $i$ th measurement,  $\vec{r}_j$  represents the location of the  $j$ th pixel, and  $\bar{E}_{Tx}$  and  $\bar{E}_{Rx}$  are the fields produced by the transmitter and receiver RISs at the location of each voxel, respectively. We solve equation (1) using computational techniques (e.g., cgs) to estimate  $\boldsymbol{\sigma}_{N \times 1}$ .

Fig. 3 depicts the imaging results for our proposed method, raster scanning, and random patterns. When raster scanning, all 6 transmitting RISs are combined as one large RIS to form a directive beam toward a target location in the ROI. The same is done for receiving RISs. We then raster scan the ROI by changing this target location. For random patterns, the reflection phase of the RISs is set randomly. The nine red targets in Fig. 3 were reconstructed using 16 masks and five frequency points ranging from 5.9 GHz to 6.1 GHz. It is evident that our method can resolve the 9 objects. However, raster scanning and random patterns do not properly reconstruct the image. Because the ROI is large, 16 scans are insufficient, and raster scanning requires additional

measurements. The random pattern also does not work with 16 masks. All results are reported for a 20dB signal-to-noise ratio.

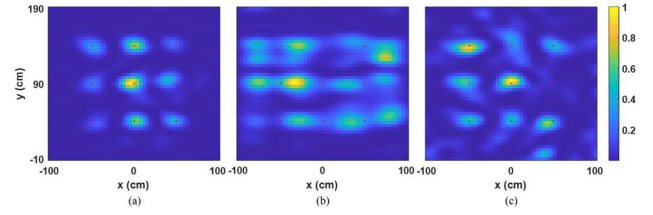


Figure 3: The imaging results for (a) our method, (b) raster scanning, and (c) random patterns. Targets are at  $z=8m$ .

In many practical implementations, one may use smaller RISs not placed close to each other. The impact of varying the spacing between the RISs ( $S_x$  and  $S_y$  in Fig. 1) is demonstrated in Fig. 4. We see that the proposed method can work even when RISs are placed apart, which can be useful in practical implementations.

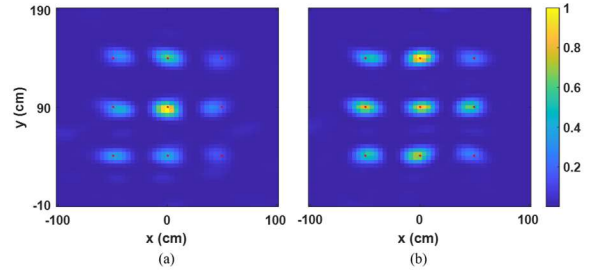


Figure 4: Imaging results using our method for (a)  $S_x=S_y=5$  cm and  $M=125$  and (b)  $S_x=S_y=10$  cm and  $M=175$ . Targets are at  $z=8m$ .

### III. CONCLUSION

In this paper, we presented a novel microwave imaging system based on RISs that combines the benefits of random patterns and spotlight imaging. Notably, the system shows robust performance even when the RISs are separated, providing greater flexibility in practical deployment. For future work, constraints on RIS elements will be introduced, and their impact on imaging will be investigated.

### ACKNOWLEDGMENT

This material is based upon work supported by the National Science Foundation under Grant No. ECCS-2333023.

### REFERENCES

- [1] Q. Wu and R. Zhang, "Towards smart and reconfigurable environment: Intelligent reflecting surface aided wireless network," *IEEE Communications Magazine*, vol. 58, no. 1, pp. 106–112, Jan. 2019.
- [2] X. Li, M. Wang, Y. Deng, and Q. Zhao, "Intelligent metasurface imager and recognizer for full-scene Wi-Fi sensing," *IEEE Transactions on Wireless Communications*, vol. 20, no. 10, pp. 6478–6489, Oct. 2021.
- [3] Z. He, X. Li, and M. Zhao, "High-resolution WiFi imaging with reconfigurable intelligent surfaces," *IEEE Internet of Things Journal*, vol. 8, no. 2, pp. 987–995, Jan. 2021.
- [4] A. V. Diebold, M. F. Imani, and D. R. Smith, "Phaseless radar coincidence imaging with a MIMO SAR platform," *Remote Sensing*, vol. 11, no. 5, p. 533, Mar. 2019.
- [5] G. Lipworth, A. Rose, O. Yurduseven, V. Gowda, M. Imani, H. Odabasi, P. Trofatter, J. Gollub, and D. R. Smith, "Comprehensive simulation platform for a metamaterial imaging system," *Applied Optics*, vol. 54, no. 31, pp. 9343–9353, Nov. 2015.